Available online at www.sciencedirect.com
ScienceDirect
Chinese Journal of Natural Medicines 2019, **17**(9): 0663–0671
Chinese Journal of Natural Medicines

Pyridocarbazole alkaloids from *Ochrosia borbonica*: lipid-lowering agents inhibit the cell proliferation and adipogenesis of 3T3-L1 adipocyte via intercalating into supercoiled DNA

XU Yao-Hao[Δ], LI Wei[Δ], RAO Yong[*], HUANG Zhi-Shu, YIN Sheng[*]

Guangdong Provincial Key Laboratory of New Drug Design and Evaluation, School of Pharmaceutical Sciences, Sun Yat-sen University, Guangzhou, Guangdong 510006, China

Available online 20 Sep., 2019

[ABSTRACT] Bioassay-guided fractionation of an ethanolic extract of *Ochrosia borbonica* led to the isolation of two known pyridocarbazole alkaloids, ellipticine (**1**) and 9-methoxyellipticine (**2**), and six known monoterpenoid indole alkaloids (**3**–**8**). Lipid-lowering assay in 3T3-L1 cell model revealed that **1** and **2** could significantly inhibit the lipid droplet formation (EC_{50} = 0.41 and 0.92 μmol·L^{-1}, respectively) and lower triglyceride levels by 50%–60% at the concentration of 1 μmol·L^{-1}, being more potent than the positive drug luteolin (EC_{50} = 2.63 μmol·L^{-1}). A mechanistic study indicated that **1** and **2** could intercalate into supercoiled DNA, which consequently inhibited the mitotic clonal expansion of 3T3-L1 cells at the early differentiation phase, leading to the retardance of following adipogenesis and lipogenesis. These findings suggest that **1** and **2** may serve as promising leads for further development of anti-obesity drugs.

[KEY WORDS] *Ochrosia borbonica*; Pyridocarbazole alkaloids; Lipid-lowering agents

[CLC Number] R965 **[Document code]** A **[Article ID]** 2095-6975(2019)09-0663-09

Introduction

Obesity is a medical condition in which excess body fat has accumulated to the extent that it may have a negative effect on health. People are generally considered obese when the body mass index (BMI), a measurement obtained by dividing a person's weight by the square of the person's height, is over 30 kg·m^{-1} [1]. Plenty of evidences have proved that obesity increases the likelihood of various diseases and conditions, particularly cardiovascular diseases, type 2 diabetes, obstructive sleep apnea, certain types of cancer, osteoarthritis and depression [2]. On average, the obesity reduces life expectancy by six to seven years. In 2013, the American Medical Association classified obesity as a disease, as it is becoming a leading preventable cause of death worldwide with increasing incidence rates annually [1]. In 2015, 711 million people are obese worldwide, and 4 million died of obese related diseases [3]. Comparing with dieting and physical exercise therapies, medication is a faster and more popular way to combat the obesity. The current anti-obesity medicines mainly include two classes: appetite inhibitors (Lorcaserin, Phentermine/topiramate, Naltrexone/amfepramone, and Liraglutide) and gastrointestinal lipase inhibitor (orlistat) [4-5]. However, the diminishing efficacy in long-term intake and associated adverse effects, such as diarrhea, mental disorders, and cardiovascular risks, restrict the clinical use of these drugs [6]. Thus, the search for novel anti-obesity agents with long-term efficacy and less side effects is compelling.

[Received on] 28-Apr.-2019

[Research funding] This work was supported by the National Natural Science Foundation of China (Nos. 81573302, 81722042, and 81703336), the Guangdong Natural Science Funds for Distinguished Young Scholar (No. 2014A0303 06047), the Science and Technology Planning Project of Guangdong Province, China (No. 2015A020211 007), the Fundamental Research Funds for the Central Universities (No. 17ykzd12), and the Guangdong Provincial Key Laboratory of Construction Foundation (No. 2017B030314030).

[*Corresponding author] Tel/Fax: 86-20-39943090, E-mail: yinsh2@mail.sysu.edu.cn (YIN Sheng); Tel: 86-20-39943068, Fax: 86-20-39943056, E-mail: raoyong0805@126.com (RAO Yong).

[Δ]These authors have contributed equally to this work.

These authors have no conflict of interest to declare.

Natural product has proved to be a valuable source of anti-obesity agents. Examples of lipid-lowering substances such as panclicins and lipstatin, and anti-obesity drug (orlistat), are all derived from natural products [7-8]. In our previous study, we also identified a natural alkaloid bouchardatine and its mimetics as potential adipogenesis/lipogenesis inhibitors for antiobesity treatment, and illustrated its mechanism on stimulation of the sirtuin 1/liver kinase B-1/AMPK axis [9]. In the continuing program aiming for the discovery of natural anti-obesity agents, we found a certain fraction of ethanolic extract of *Ochrosia borbonica* exhibited potent lipid-lowering effects.

Ochrosia borbonica Gmelin (Apocynaceae) is an arbor tree widely distributed in Southeast Asia [10]. Previous chemical investigations of this plant led to the isolation of several indole alkaloids, sterols, and triterpenoids, some of which showed cytotoxic and anti-inflammatory activities [11−13]. In the current study, the chemical investigation of lipid-lowering fraction of *O. borbonica* led to the isolation of two known pyridocarbazole alkaloids, ellipticine (**1**) and 9-methoxyellipticine (**2**), and six known monoterpenoid indole alkaloids (**3**–**8**). Herein, we reported the verification of the lipid-lowering activities of **1** and **2** and their potential action mechanism.

Results and Discussion

Bioassay-Guided isolation of compounds 1–8

The air-dried powder of leaves of *O. borbonica* was extracted with 95% EtOH at room temperature to give a crude extract, which was suspended in H_2O and partitioned successively with petroleum ether, EtOAc, and *n*-BuOH. Each fraction was tested for its inhibitory effect on the lipid droplet formation in 3T3-L1 cells, and the EtOAc fraction with *ca.* 70% inhibition at 100 μg·mL^{-1} was selected for further chemical investigation. Subsequent purification of this fraction using various chromatographic methods led to the identification of eight known alkaloids (**1**–**8**, Fig. 1). These alkaloids were identified as ellipticine (**1**), 9-methoxyellipticine (**2**) [14], apparicine (**3**) [15], 10-methoxyapparicine (**4**) [16], 15α-hydroxy-10-methoxyapparicine (**5**) [12], pleiocarpamine (**6**) [17], (2*S*, 3*S*, 15*S*, 19*S*, 20*S*)-isoreserpiline pseudoindoxyl (**7**) [18], isoreserpiline (**8**) [19], by comparison of their physical and spectroscopic data ([α]$_D$, ^{1}H and ^{13}C NMR, ESIMS) with those reported in the literature.

The lipid-lowering and cell cycle arrest effects of 1 and 2 in 3T3-L1 adipocyte model

To verify the lipid-lowing ability of these isolates, **1**–**8** were subjected to Triglyceride assay in 3T3-L1 adipocyte model. The results showed that **1** and **2** significantly decreased the formation of lipid droplet by *ca.* 80% at 10 μmol·L^{-1}, while other compounds decreased the lipid formation by no more than 40%. Thus, **1** and **2** were selected as promising candidates for further study. As shown in Fig. 2A, within the concentrations of 0.01−10 μmol·L^{-1}, **1** and **2** efficiently reduced the formation of lipid droplet in a dose-dependent manner, with EC_{50s} being at 0.41 and 0.92 μmol·L^{-1}, respectively, which are more potent than the natural lipid-lowering agent luteolin (EC_{50} = 2.63 μmol·L^{-1}).

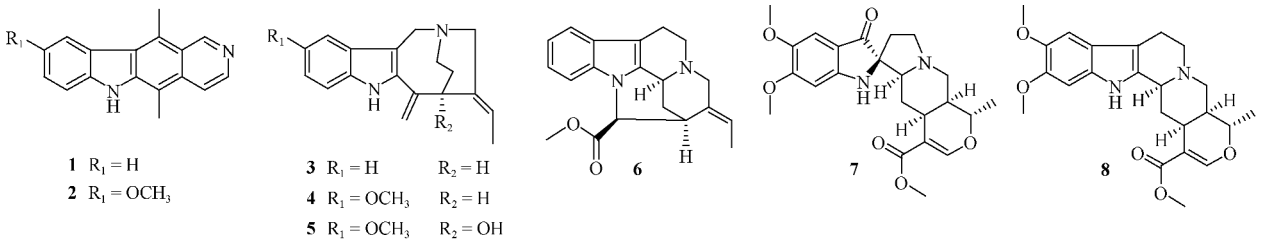

Fig. 1 The structure of compounds 1–8

3T3-L1 cells would undergo a necessary and multi-step differentiation process transforming from preadipocytes to mature white adipocytes to start adipogenesis. This process can be divided into 3 phases, namely adipogenesis (0–3 days), lipogenesis (3–6 days), and terminal differentiation stage (6–9 days) [20-21]. Thus, the modulations of **1** and **2** on the differentiation process of 3T3-L1 were investigated in different time spans. As shown in Fig. 2B, the treatments of **1** and **2** at 1 μmol·L^{-1} in the early phase of the differentiation (0–3 days) significantly decreased the triglyceride levels in 3T3-L1, while the prolonged treatments of **1** and **2** (0–6 or 0–9 days) didn't show much improvement of the inhibition. Meanwhile, the later **1** and **2** intervened (3–6 or 6–9 days), the less efficacy they exerted. This was further confirmed by Oil Red O Staining experiments (Fig. 2C), the formation of lipid droplets were effectively retarded when **1** and **2** were treated in 0–3 days at 1 μmol·L^{-1}, while the treatments of **1** and **2** in 3–6 days or 6–9 days only slightly inhibited the lipid formation. These results suggested that **1** and **2** exerted their lipid- lowering effects at the early phase of the cell differentiation (0–3 days).

As mitotic clonal expansion (MCE) is a necessary process in 3T3-L1 adipogenesis, which activates the post-confluent cells to reenter the cell cycle and to initiate the process of adipogenesis, a cell cycle analysis on 3T3-L1 adipocytes were studied by flow cytometry to verify the interruption of **1** and **2** on the MCE process. As shown in Fig. 3A, the treatments of **1** and **2** induced a decrease of the ratio of S phase in a dose-dependent manner, while the ratios of G0/G1 and G2/M phase were increased correspondingly. Meanwhile, the treatments of **1** and **2** efficiently inhibited cell proliferation in a time course as compared with control cells (Fig. 3B), indicat-

ing that **1** and **2** could block the MCE in adipogenesis. As **1** and **2** were previously reported as anti-cancer agents [22-23], their lipid-lowering effects in current study may be due to intrinsic cytotoxicity. To exclude this possibility, the cytotoxicity of **1** and **2** in 3T3-L1 adipocytes was evaluated by lactate dehydrogenase (LDH) releasing assay. As shown in Fig. 3C, the treatments of **1** and **2** within the concentrations of 0.01–10 μmol·L^{-1} did not alter the releasing levels of LDH, indicating that **1** and **2** could exert the lipid-lowering effect at a safe dose (1 μmol·L^{-1}) before inducing certain cytotoxicity.

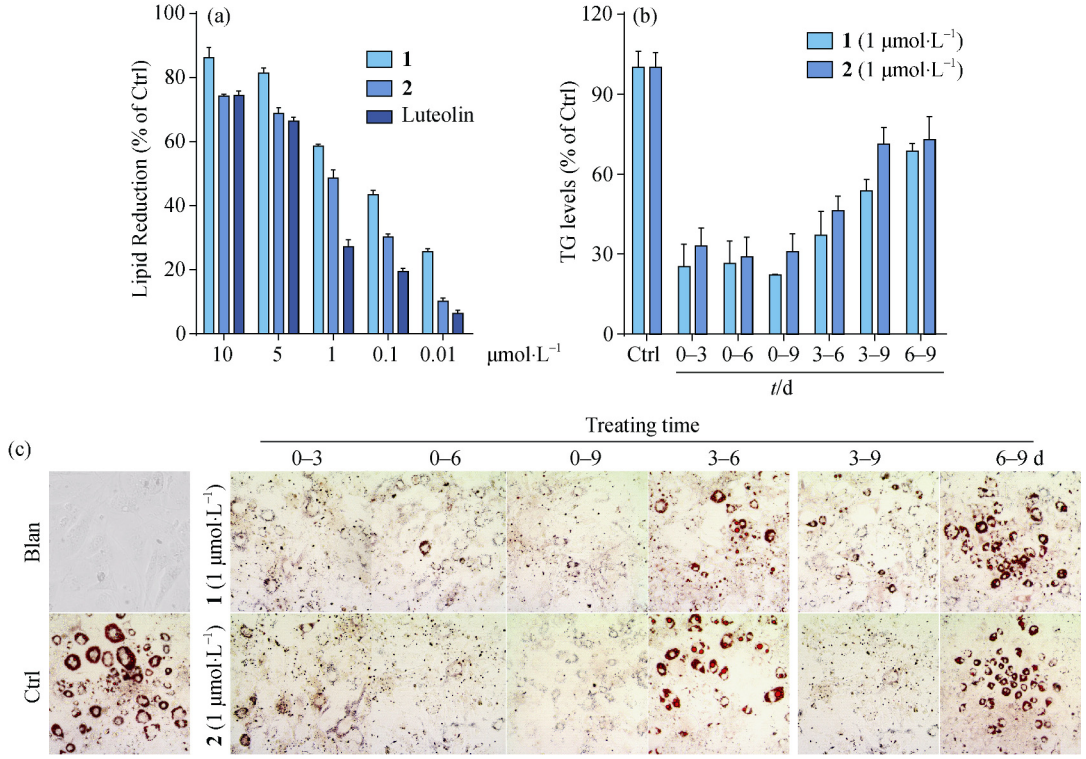

Fig. 2 Evaluation of the lipid-lowering effects of 1 and 2 in 3T3-L1 adipocyte model. (A) The lipid reduction ratios were determined with the treatments of different doses of 1, 2, and luteolin. (B) The triglyceride levels were determined by a TG assay with the treatments of 1 and 2 at 1 μmol·L^{-1} on different differentiation stages. (C) Images of lipid droplet formation stained by Oil Red O were captured with the treatments of 1 and 2 at 1 μmol·L^{-1} on different differentiation stages

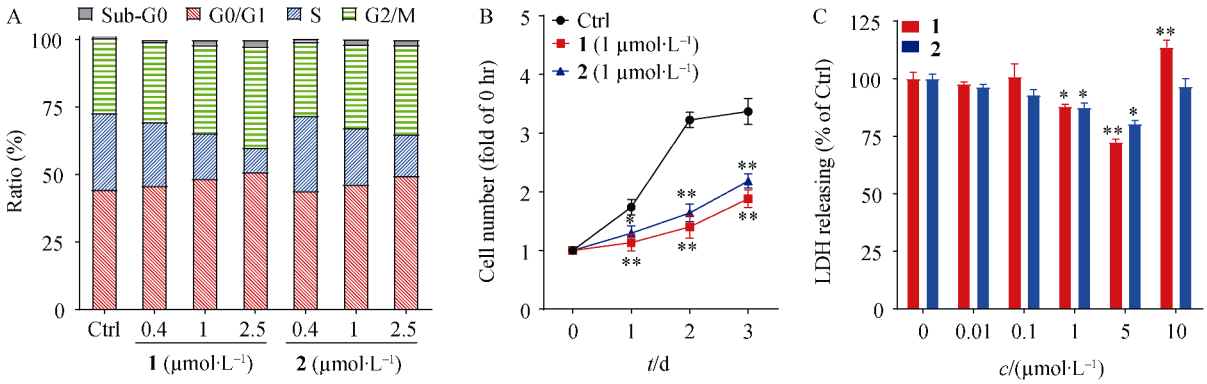

Fig. 3 Compounds 1 and 2 inhibited the MCE activity in 3T3-L1 adipocytes without inducing cell cytotoxicity. (A) Cell cycle analysis by flow-cytometry. After 24 h, cells were harvested and fixed with 70% ice-cold methanol overnight, and then subjected to cycling analysis by flow cytometry method for DNA content. (B) Cell number analysis by hemacytometer analyzer. 3T3-L1 adipocytes were treated with 1 or 2 (1 μmol·L^{-1}) for 0, 24, 48, 72 h, cell numbers were counted by hemacytometer analyzer at each time point, respectively, the data were calculated and the growth curve were presented as fold of 0 h. (C) Cell cytotoxicity analysis by LDH assay. After 24 h incubation, the culture medium were collected and centrifuged at 3000 *g* for 5 min, the supernatant were subjected to LDH releasing assay as depicted in Materials and Methods. $^{*}P < 0.05$, $^{**}P < 0.01$ *vs* ctrl group, $n = 3$ independent experiments

*Inhibitory effects of **1** and **2** on Top I-and II-catalyzed DNA unwinding.*

As topoisomerases play the important roles in DNA replication, and contribute to the early steps of adipogenesis in 3T3-L1 cells [24], the inhibition of **1** and **2** on Top I and II was evaluated by DNA unwinding assays. The Top I inhibitor camptothecin (CPT) and Top II inhibitor etoposide (VP-16) were used as positive controls, respectively [25-26]. As showed in Fig. 4A, pBR322 DNA kept in supercoiled state (Sc) in blank group, while the treatment of top I uncoiled the supercoiled pBR322 DNA to relaxed state (Rx) in control group. The treatments of **1** and **2** with increasing doses gradually inhibited the Top I-induced unwinding effect and retained pBR322 DNA in supercoiled state in a dose-depend manner. These inhibitory effects were comparable to that of CPT, and **1** showed better activity than **2**. Similar inhibitory effects of **1** and **2** on Top II were also observed as shown in Fig. 4B. These results suggested that **1** and **2** may inhibit the Top I-and II-catalyzed DNA unwinding *in vitro*, which were consistent with the inhibitory effects on cell cycle in 3T3-L1 adipocytes.

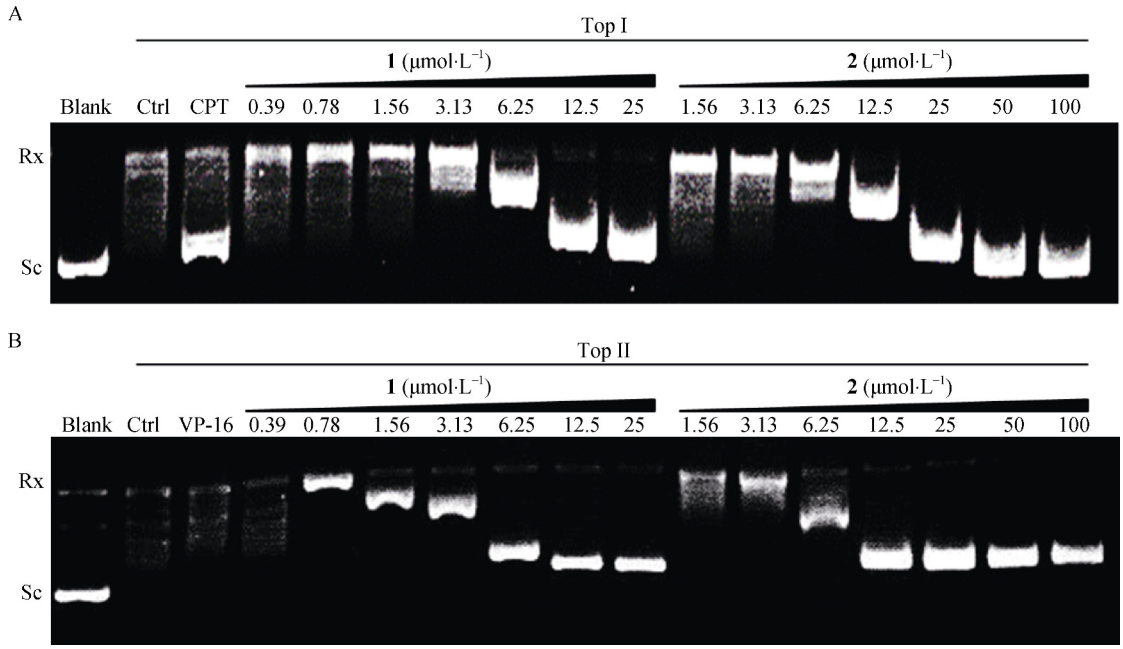

Fig. 4 The inhibitory effects of 1 and 2 on Top I-and II-catalyzed DNA unwinding. (A) Top I inhibition of 1 and 2. Lane 1: pBR322 DNA, Lane 2: pBR322 DNA + Top I, Lane 3: pBR322 DNA + Top I + 100 μmol·L^{-1} CPT, Lane 4–10: pBR322 DNA + Top I + 1 (0.39, 0.78, 1.56, 3.13, 6.25, 12.5, 25 μmol·L^{-1}), Lane 11–17: pBR322 DNA + Top I + 2 (1.56, 3.13, 6.25, 12.5, 25, 50, 100 μmol·L^{-1}). (B) Top II inhibition of 1 and 2. Lane 1: pBR322 DNA, Lane 2: pBR322 DNA + Top II, Lane 3: pBR322 DNA + Top I + 100 μmol·L^{-1} VP-16, Lane 4–10: pBR322 DNA + Top II + 1 (0.39, 0.78, 1.56, 3.13, 6.25, 12.5, 25 μmol·L^{-1}), Lane 11–17: pBR322 DNA + Top II + 2 (1.56, 3.13, 6.25, 12.5, 25, 50, 100 μmol·L^{-1}). *n* = 3 independent experiments

*DNA binding properties of **1** and **2***

The inhibition of **1** and **2** on Top I-and II-catalyzed DNA unwinding may involve two action mechanisms: compounds directly targeted Tops, leading to the inactivation of the enzymes, or intercalated into the Topoisomerase' substance, DNA, stabilizing the DNA-Tops complex in a supercoiled state. To clarify the accurate action mode, the DNA unwinding assay and ethidium bromide (EB) displacement experiment were carried out. EB is a well-known DNA intercalator which could induce Top I to twist relaxed DNA into a supercoiled state. Meanwhile, CPT, a Top I inhibitor specifically targeting enzyme, would not affect the state of the relaxed DNA. If the treatment of compounds with Top I and relaxed DNA generates the supercoiled DNA, **1** and **2** are supposed to be DNA intercalators, otherwise **1** and **2** are supposed to be Topoisomerase inhibitors. As shown in Fig. 5, pBR322 DNA remained in a relaxed state (Rx) in both blank and 100 μmol·L^{-1} CPT groups, while the treatments of EB with the presence of Top I gradually transformed relaxed DNA into supercoiled stated in a dose-dependent manner (0.5–2.5 μmol·L^{-1}). The treatments of **1** or **2** with different doses (3.13–50 μmol·L^{-1}) exhibited the similar Top I-induced twisting effects with EB, indicating that they shared the same action mode, acting as DNA intercalators. This was further confirmed by EB fluorescence displacement experiments. When EB intercalates into DNA, the EB-DNA complex will generate a characteristic fluorescence at the wavelength of 590 nm. The intensity of fluorescence is in proportion to the concentration of DNA. When other intercalators competitively displace EB from the complex, the fluorescence will be decreased. Firstly, an absorption spectra model with the presence of 1 μmol·L^{-1} EB and different doses of DNA was built to optimize a

suitable DNA concentration. As shown in Fig. 5B, when the DNA concentrations increased from 2 to 12 μM, the fluorescence intensity gradually reached maximum, indicating that the interaction between EB and DNA reached saturated at about 12 μmol·L^{-1}. Thus, this DNA concentration was chosen for next displacement assay. As shown in Fig. 5C−5E, the treatments of **1** or **2** in EB-DNA complex decreased the fluorescence intensity, and the hypochromicity was in a dose- dependent manner at the range of 0.01−100 μmol·L^{-1}.

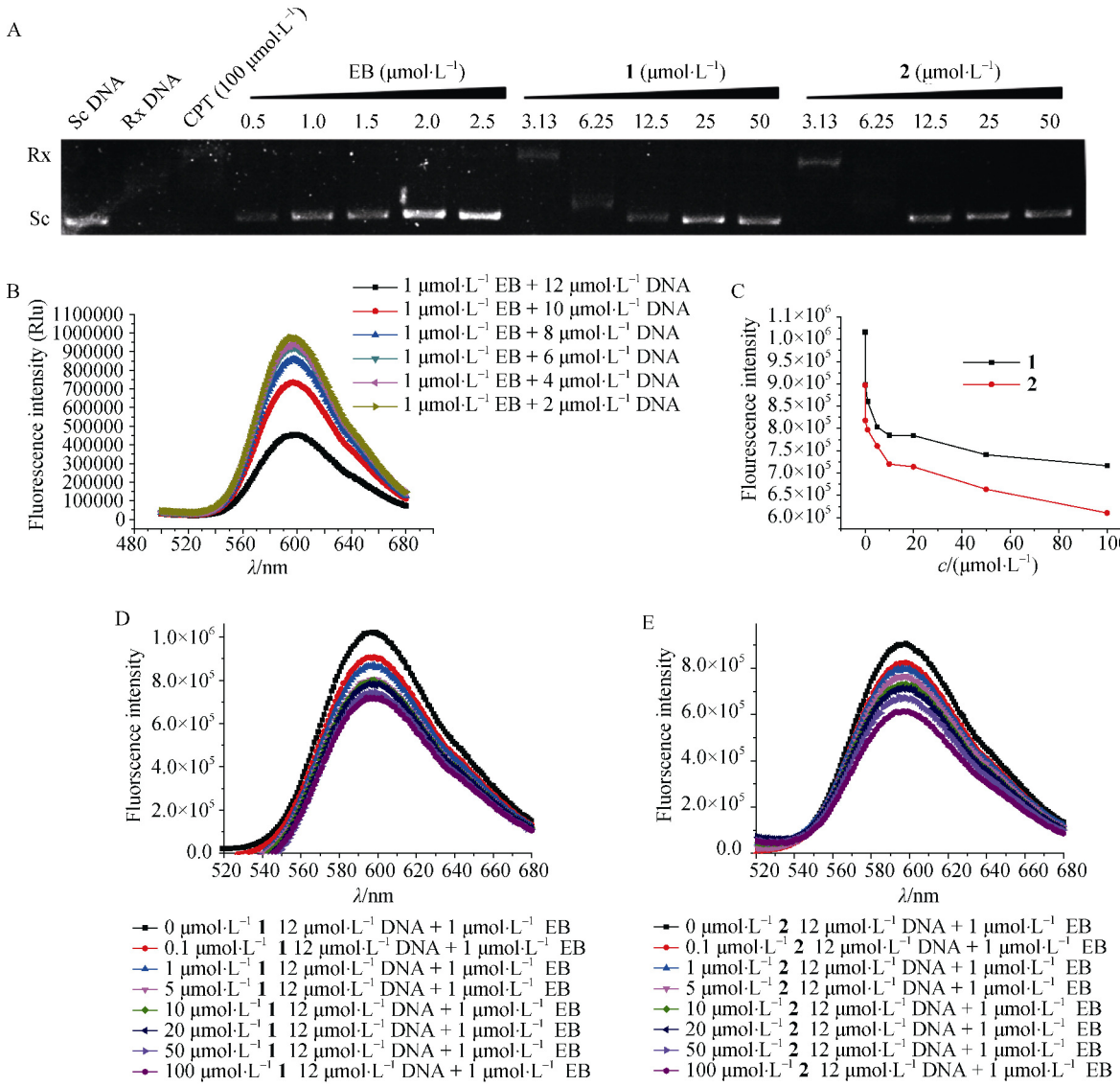

Fig. 5 Determination the DNA binding properties of 1 and 2. (A) Agarose gel electrophoresis of relaxed pBR322 DNA containing increasing concentration of EB and tested compounds. Lane 1: Supercoiled DNA (Sc DNA), Lane 2: Relaxed DNA (Rx DNA) + Top I, Lane 3: Rx DNA + CPT (100 μmol·L^{-1}) + Top I, Lane 4–8: Rx DNA + Top I + EB (0.5, 1, 1.5, 2, 2.5 μmol·L^{-1}), Lane 9–13: Rx DNA + Top I + 1 (3.13, 6.25, 12.5, 25, 50 μmol·L^{-1}), Lane 14–18: Rx DNA + Top I + 2 (3.13, 6.25, 12.5, 25, 50 μmol·L^{-1}). (B–E) Absorbance spectrum of CT-DNA with different compounds. (B) 1 μmol·L^{-1} EB titrated by increasing concentration of DNA. (C) The curve formed by the maximum absorbance spectrum of difference concentration of 1 or 2. (D) 12 μmol·L^{-1} DNA bound by 1 μmol·L^{-1} EB titrated by increasing concentration of 1. (E) 12 μmol·L^{-1} DNA bound by 1 μmol·L^{-1} EB titrated by increasing concentration of 2

Taken together, compounds **1** and **2** could intercalate into DNA, and their intercalating activity was weaker than that of EB.

Intranuclear DNA damage properties of 1 and 2

As **1** and **2** could intercalate into DNA, their intracellular DNA damage properties were expected. To verify this, the DNA damage marker, γH_2X, was detected in 3T3-L1 cells with the treatments of **1** or **2** by western blot. As shown in Fig. 6A, **1** and **2** significantly upregulated the γH2X level when

treated for 15 h or 24 h, and this damage effect was in a dose-dependent manner (0.4–2.5 μmol·L^{-1}). This was further confirmed by immunofluorescence assay, in which a well-known DNA-damaging agent, cisplatin, was used as the positive control. As shown in Fig. 6B, the generation of γH2X was obviously spotted in the nuclear of 3T3-L1 cells when treated with **1** or **2** at 1 μmol·L^{-1} for 24 h. This phenomenon was similar to the cisplatin-induced DNA damage, revealing DNA damage properties of **1** and **2**, which further evidenced the DNA intercalating activity of **1** and **2**.

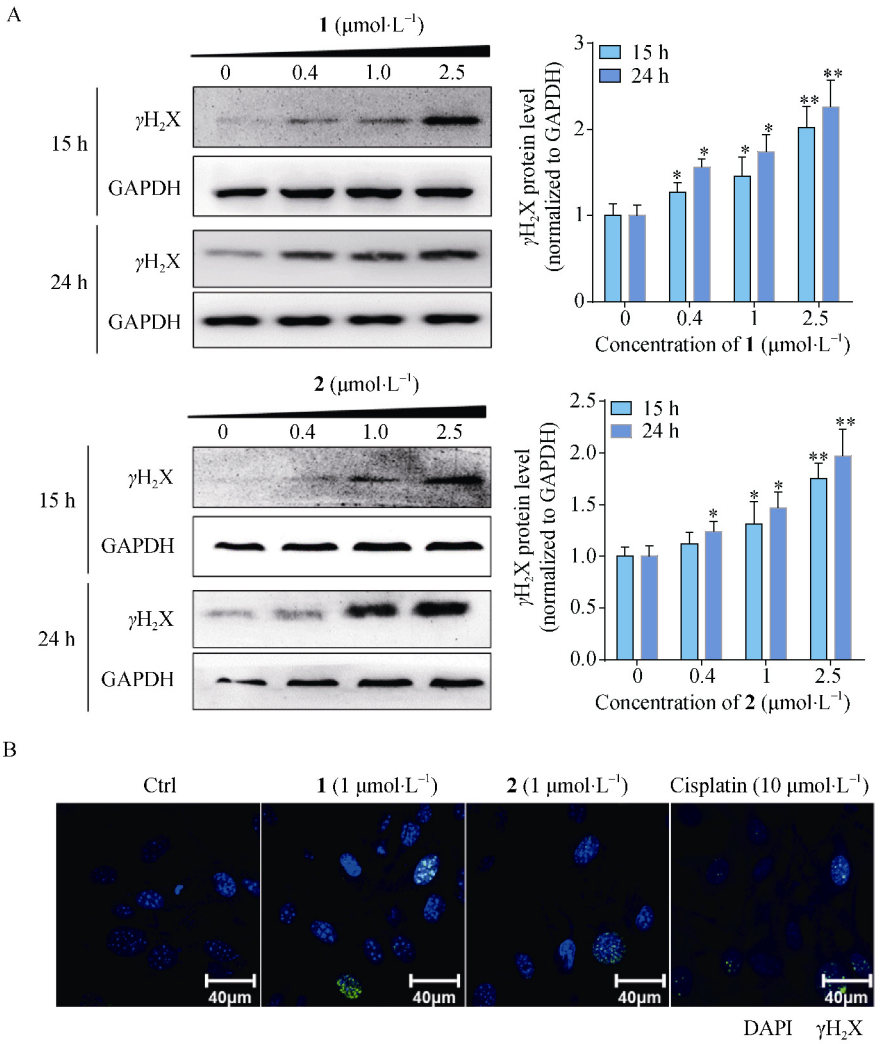

Fig. 6 Compounds 1 and 2 induced DNA damage. 3T3-L1 cells were treated with 1 and 2 for 15 or 24 h, respectively. Then cells were collected and subjected to SDS-PAGE for indicated proteins analysis by western blot. (A) Expression levels of protein γH$_2$X in 3T3-L1 cells with the treatments of 1 and 2, and protein levels were quantified by quantity one software. (B) Protein level of γH$_2$X determined by immunofluorescence after 24 h treatment. $^{*}P < 0.05$, $^{**}P < 0.01$ *vs* ctrl group, $n = 3$ independent experiments

Pyridocarbazole alkaloids are a group of rare natural products mainly occurring in the plants of family Apocynaceae. Since ellipticine and olivacine were first isolated in the late 1950s, the intriguing structures and pronounced antitumor activity of this compound class have attracted considerable interests from both chemists and pharmacologists over the last half century. In the current study, the lipid-lowering activity of pyridocarbazole alkaloids ellipticine (**1**) and 9-methoxyellipticine (**2**) were reported for the first time. Compounds **1** and **2** could significantly inhibit the lipid droplet formation and lower triglyceride levels at the concentration of 1 μmol·L^{-1}, without inducing apparent cytotoxicity. A mechanistic study revealed that compounds **1** and **2** exerted its lipid-lowering effect by blocking the MCE activity during the early phase of 3T3-L1 differentiation. They could intercalate into Topoisomerase-targeted DNA, leading to DNA damage and consequent cell cycle arrested and cell proliferation inhibition. These properties may make them promising lead structures for the development of anti-obesity agents.

Experimental

General experimental procedures

Optical rotations were measured on a Rudolph Autopol I automatic polarimeter, NMR spectra were measured on a

Bruker AM-400 spectrometer at 25 °C. ESIMS was measured on a Finnigan LCQ Decainstrument. A Shimadzu LC-20 AT equipped with an SPD-M20A PDA detector was used for HPLC. A YMC-pack ODS-A column (250 mm × 10 mm, S-5 μm, 12 nm) was used for semi-preparative HPLC separation. Silica gel (300–400 mesh, Qingdao Haiyang Chemical Co., Ltd.), C_{18} reversed-phase (RP-C_{18}) silica gel (12 nm, S-50 μm, YMC Co., Ltd.), and Sephadex LH-20 gel (Amersham Biosciences) were used for column chromatography (CC). All solvents were of analytical grade (Guangzhou Chemical Reagents Company, Ltd.).

Plant material

The leaves of *Ochrosia borbonica* were collected in February 2014 at Guangzhou city, Guangdong Province, Republic of China, and authenticated by Prof. XU You-Kai, Xishuangbanna Tropical Botanical Garden, Chinese Academy of Sciences. China. A voucher specimen (accession number: YBL 201402) has been deposited at the School of Pharmaceutical Sciences, Sun Yat-sen University, Guangzhou, China.

Extraction and isolation

The air-dried powder leaves of (5 kg) of *O. borbonica* were extracted with EtOH (3 × 2 L) at rt to give 400 g of crude extract. The extract was suspended in H_2O (400 mL) and partitioned sequentially to give dried petroleum ether (110 g) and EtOAc (90 g) extracts. The EtOAc extract was subjected to MCI gel CC eluted with a MeOH/H_2O gradient (2 : 8→10 : 1) to afford Fr. I–IV. Separation of the Fr. I (8 g) was purified on Sephadex LH-20 CC (CH_2Cl_2/MeOH, 1 : 1) to give Fr. Ia–Ic. Fr. Ia was purified using HPLC (MeOH/H_2O, 80 : 20, 3 mL·min^{-1}) to give **6** (9 mg, t_R 14 min). Fr. Ib (35 mg) was subjected to silica gel CC (MeOH/CH_2Cl_2, 1 : 100) to give **3** (11 mg), and Fr. Ic (120 mg) was purified on silica gel CC (MeOH/CH_2Cl_2, 1 : 30) to produce **4**. Fr. II (11 g) was subjected to Sephadex LH-20 CC eluted with MeOH to give Fr. IIa–IId. Fr. IIa was followed by HPLC (MeOH/H_2O, 75 : 25, 3 mL·min^{-1}) to yield **7** (16 mg, t_R 11 min). Fr. IIc was purified using HPLC (MeCN/H_2O, 77 : 13, 3 mL·min^{-1}) to obtain **8** (350 mg, t_R 13.5 min). Fr. IV was chromatographed loaded on C_{18} reversed-phase (RP-18) silica gel eluted with MeOH/H2O (4 : 6→10 : 0) to obtain Fr. IVa–IVc. Fr. IVa was further purified HPLC (MeOH/H_2O, 95 : 5, 3 mL·min^{-1}) to yield **1** (50 mg, t_R 18 min) and **2** (75 mg, t_R 19.5 min). Further purification of Further purification of Fr. IVb was conducted by silica gel CC (MeOH/CH_2Cl_2, 1 : 20) to produce **5** (180 mg). The purity of compounds **1**–**8** was estimated to be greater than 95%, as determined by their ^{1}H NMR spectra.

Cell culture

Mouse 3T3-L1 fibroblast cells were purchased from Type Culture Collection (ATCC, Rockefeller, Maryland, USA). Cells were maintained in DMEM supplemented with 10% FBS, penicillin (100 U·mL^{-1}) and streptomycin (100 μg·mL^{-1}). For the MTT assay and LDH assay, 3T3-L1 cells were plated at a density of 2 × 10^3 per well in 96-well microplates. Cells were cultured until merged. Compounds **1** and **2** were added to the wells at increasing concentrations (0, 0.01, 0.1, 1, 5, 10 μmol·L^{-1}) with the culture medium containing 500 mmol·L^{-1} IBMX (3-isobutyl-1-methylxanthine), 4 mg·mL^{-1} Insulin and 1 mg/mL Dexamethason.

Top I inhibitory activity

The effects of compounds on DNA relaxation catalyzed by DNA Top I (TaKaRa, Kyoto, Japan) were determined by measuring the relaxation of supercoiled DNA pBR322 (TaKaRa, Kyoto, Japan) using camptothecin as a positive control. The reaction mixture was prepared according to the provided protocol, and incubated at 37 °C for 30 min. The reactions were terminated by the addition of dye solution containing 1% SDS, 0.02% bromophenol blue and 50% glycerol. The mixtures were applied to 1% agarose gel and subjected to electrophoresis for 1 h, in TAE buffer (40 mmol·L^{-1} Tris-acetate, 2 mmol·L^{-1} EDTA). Gels were stained for 30 min in 60 mL 1 × TAE buffer with 2 μL Gel Red. DNA bands were visualized by transillumination with UV light and then photographed by Alpha Innotech digital imaging system.

Top II inhibitory activity

We used the Top II assay kit from Top GEN to determine the effects of compounds on DNA relaxation catalyzed by human Top II. Relaxation assays were carried out according to the manufacturer's instructions with minor modifications. The assay was performed in a final volume of 20 μL in Top II reaction buffer (1 × Top II buffer = 50 mmol·L^{-1} Tris-HCl, pH 8.0, 150 mmol·L^{-1} NaCl, 10 mmol·L^{-1} $MgCl_2$, 2 mmol·L^{-1} ATP, 0.5 mmol·L^{-1} dithiothreitol, and 30 mg·mL^{-1} BSA) with 0.2 mg pBR322 DNA. Compounds were included in the reactions at a constant solvent volume. Reactions were initiated by addition of 1U human Top IIα, and incubated for 30 min at 37 °C. Reaction was terminated with 5 × stop buffer (5 mL per 20 mL reaction volume). Stop buffer contained 5% sarkosyl, 0.0025% bromophenol blue and 25% glycerol. Reaction products were analyzed on a 1% agarose gel in TAE buffer (40 mmol·L^{-1} Tris-acetate, 2 mmol·L^{-1} EDTA). Gels were stained for 30 min in 60 mL 1 × TAE buffer with 2 μL Gel Red DNA bands were visualized through transillumination with UV light and then photographed by Alpha Innotech digital imaging system.

Topoisomerase I DNA unwinding Assay

Relaxed pBR322 plasmid DNA utilized in unwinding assays was generated by treating negatively supercoiled pBR322 with topoisomerase I in topoisomerase I reaction buffer (50 mmol·L^{-1} Trise-HCl, pH 7.5, 50 mmol·L^{-1} KCl, 10 mmol·L^{-1} $MgCl_2$, 0.5 mmol·L^{-1} DTT, 0.1 mmol·L^{-1} EDTA, and 30 mg·mL^{-1} bovine serum albumin) prior to the addition of other reaction components. Assay mixtures contained 0.1 mg relaxed pBR322 plasmid DNA, topoisomerase I (10 U), and compounds in 20 μL of topoisomerase I reaction buffer. Following a 10 min incubation of DNA and compound at room temperature, topoisomerase I was added, and reactions

were incubated for 30 min at 37 °C. Reactions were stopped by adding an equal volume of phenol chloroform. Aqueous samples (20 μL) were removed from the reactions, and 3 mL of stop solution (0.77% SDS, 77 mmol·L^{-1} NaEDTA, pH 8.0) followed by 2 mL of agarose gel loading buffer (30% sucrose, in 10 mmol·L^{-1} Tris-HCl, pH 7.9) was added to each. Samples were subjected to electrophoresis in a 1% agarose gel in TAE buffer (40 mmol·L^{-1} Tris-acetate, 2 mM EDTA). DNA bands were stained with an aqueous solution of ethidium bromide (0.5 mg·mL^{-1}), visualized with UV light, and photographed by Alpha Innotech digital imaging system.

Oil Red O staining and measuring the lipid content

Oil Red O staining was performed using the following procedure. The cells were washed with ice-cold PBS buffer (0.2 mol·L^{-1} NaCl, 10 mmol·L^{-1} Na_2HPO_4, 3 mmol·L^{-1} KCl, and 2 mmol·L^{-1} KH_2PO_4, pH 7.4) and then fixed with 4% formaldehyde (*V*/*V*) for 1 h at room temperature followed by three washes with distilled water. The cells were stained with freshly prepared Oil Red O working solution for 30 min at room temperature and washed three times with distilled water. The plates were scanned using an OLYMPUS CKX41 microscope and camera (OLYMPUS). The Oil Red O working solution was prepared by mixing 6 mL of 0.5% Oil Red O (*W*/*V*, Sigma) in isopropanol with 4 mL of ddH_2O followed by filtration through a 0.22 μm filter (Millipore). The lipid content of the cells was measured by extracting the Oil Red O from the stained cells with 100% isopropyl alcohol and obtaining the optical density at 510 nm.

Triglyceride assay

After treatment, the cells were collected and washed three times with PBS (pH 7.4). Then, the cells were lysed with distilled water containing 0.2% Triton X-100 (MP, 194854) for 1 h at room temperature and then ultrasonicated for 15 min. The lysates were collected and centrifuged at 4 °C, 12 000 *g* for 15 min. The cholesterol and triglyceride contents of the cells were measured using GPO-POD assay kits and cholesterol analysis kits (Jiancheng Bio, China), and the protein levels were determined using BCA protein assay kits (Pierce, USA). Then, the results were expressed as "mmol triglyceride (cholesterol)/g protein" as previously described [9].

Lactate Dehydrogenase (LDH) releasing assay

After treatment, culture medium were collected and centrifuged at 3000 *g* for 5 min, the supernatants were subjected to LDH determination according to the manuscripts.

Cell growth inhibition assay

After treatment, cells were collected and resuspended in PBS. The cell suspension was mixed 1 : 1 with 0.4% Trypan Blue Stain (Jiangsu, China, Beyotime) and allowed to incubate for 5 minute at room temperature. The hemocytometer was filled with 10 μL of cell mixture, and the cells were counted.

Cell cycle analysis

After treatment, cells were harvested and fixed with 70% ice-cold methanol overnight, and then subjected to cycling analysis by flow cytometry method for DNA content.

Cell viability assay

After 0 h, 24 h, 48 h and 72 h incubation, each well were treated with 10 μL of 5 mg·mL^{-1} MTT [3-(4, 5-dimethylthiazol-2-yl) 2, 5-diphenyl-2H-tetrazolium-bromide] solution, and the cells were further incubated at 37 °C for another 4 h. At the end of the incubation, the untransformed MTT was removed, and 100 μL DMSO was added. The microplates were well shaken to dissolve the formazan dye, and the absorbance at 490 nm was measured using a microplate-reader (Bio-Tek). Both compounds does were parallel tested in triplicate, and the IC_{50} values were derived from the mean *OD* values of the triplicate tests versus compound concentration curves.

Immunofluorescence and confocal microscopy

Confocal microscopy was performed in an inverted microscope (Leica Microsystems, solmos, Germany). Cells were washed with ice-cold PBS (at pH 7.4) and then fixed with 4% paraformaldehyde for 10 min at room temperature. The fixed cells were blocked by 5% goat serum (Bioss, Beijing, China) in PBS for 2 h at room temperature and then stained with a specific first antibody of γ-H2X 1 : 50 at 4 °C overnight. After staining with an appropriate Alexa Fluor-conjugated secondary antibody for 2 h at 37 °C, the images were captured (magnification, × 400). Imaging analyses were performed using an LSM 510 laser confocal microscope (Zeiss, Jena, Germany).

Western blot analysis

3T3-L1 cells were incubated with **1** or **2** for different times (15 or 24 h), washed with PBS and resuspended in RIPA lysis buffer. After 15 min of mixing at 4 °C, the mixture was centrifuged at 12 000 × *g* for 20 min, and the supernatant was collected as whole-cell extract. Protein concentration in cell lysates was determined by the BCA assay. For Western blot analysis, equal amounts of protein was loaded and separated by 10% SDS-PAGE electrophoresis, and transferred to PVDF membrane. After transfer, the membrane was blocked in 5% bovine serum albumin in TBS buffer (10 mmol·L^{-1} Tris/HCl, 150 mmol·L^{-1} NaCl, pH 8.0) and washed in TBST buffer (TBS buffer containing 0.05% Tween-20). The membrane was incubated with primary γH2X antibodies diluted in TBST at 1 : 1000 for 12 h at 48.0) and washed in TBST buffer (TBS buffer containing 0.05% Tween-20). The membrane was incubated with primary γHr 1 h at room temperature. Result was revealed by the ECL kit (Sangon Biotech, Shanghai).

UV-vis titration

The DNA preparation and absorbance titration experiment was performed as previously described. We used EB from 2 to 12 μmol·L^{-1} to ensure the binding of DNA and EB. Next we individually added compounds **1** and **2** from 0.1 to 100 μmol·L^{-1} into CT-DNA with 10 μmol·L^{-1} EB and teat the change of the curve.

Statistical analysis

Results are expressed as the mean ± SEM. Data between two groups were analysed by Student's *t*-test using Graphpad Prism (Graphpad Software Inc, California, USA). A *P* value

of < 0.05 was considered statistically significant.

References

[1] Pollack A. AMA recognizes obesity as a disease [EB/OL]. (2013-Jun.-19) [2018-Jul.-02]. http: // www.nytimes.com/2013/06/19/business/ama-recognizesobesity-as-a-disease.html

[2] Eckel RH, Alberti K, Grundy SM, *et al*. The metabolic syndrome [J]. *The Lancet*, 2010, **375**(9710): 181-183.

[3] Collaborators GO. Health effects of overweight and obesity in 195 countries over 25 years [J]. *N Engl J Med*, 2017, **377**(1): 13-27.

[4] Greenway FL, Bray GA. Combination drugs for treating obesity [J]. *Curr Diabetes Rep*, 2010, **10**(2): 108-115.

[5] Kaplan LM. Pharmacologic therapies for obesity [J]. *Gastroenterol Clin North Am*, 2010, **39**(1): 69-79.

[6] Bray GA, Frühbeck G, Ryan DH, *et al*. Management of obesity [J]. *Lancet*, 2016, 387(10031): 1947-1956.

[7] Vermaak I, Viljoen AM, Hamman JH. Natural products in anti-obesity therapy [J]. *Nat prod Rep*, 2011, **28**(9): 1493-1533.

[8] Al DLG, Milagro FI, Boque N, *et al*. Natural inhibitors of pancreatic lipase as new players in obesity treatment [J]. *Planta Med*, 2011, **77**(8): 773-785.

[9] Rao Y, Yu H, Gao L, *et al*. Natural alkaloid bouchardatine ameliorates metabolic disorders in high-fat diet-fed mice by stimulating the sirtuin 1/liver kinase B-1/AMPK axis [J]. *Br J Pharmacol*, 2017, **174**(15): 2457-2470.

[10] Flora of China Editorial Committee. *Flora of China* [M]. Beijing: Science Press. **1977**, **63**: 39.

[11] Svoboda GH, Poore GA, Montfort ML. Alkaloids of *Ochrosia maculata* Jacq. (*Ochrosia borbonica* Gmel.). Isolation of the alkaloids and study of the antitumor properties of 9-methoxyellipticine [J]. *J Pharm Sci*, 1968, **57**(10): 1720-1725.

[12] Zhang BJ, Yan JM, Wu ZK, *et al*. Alkaloids from *Ochrosia borbonica* [J]. *Helv Chim Acta*, 2013, **96**(12): 2288-2298.

[13] Liu YP, Huang LG, Li KK, *et al*. Studies on non-alkaloid constituents from *Ochrosia borbonica* [J]. *Chin Tradit Herb Drugs*, 2015, **46**(6): 798-802.

[14] Ahond A, Popat C, Potier P. Étude par rm^{13}c d'alcaloïdes à squelette acridinone 9(10h) et pyrido(4, 3b) carbazole(6h) [J]. *Tetrahedron*, 1978, **34**(15): 2385-2388.

[15] Van Beek TA, Verpoorte R, Svendsen AB. Isolation and synthesis of vobparicine, a novel type dimeric indole alkaloid [J]. *Tetrahedron Lett*, 1984, **25**(19): 2057-2060.

[16] Akhter L, Brown RT, Moorcroft D. 10-Hydroxy- and 10-methoxyapparicine: two new alkaloids from *Ochrosia oppositifolia* [J]. *Tetrahedron Lett*, 1978, **19**(43): 4137-4140.

[17] Sauerwein M, Shimomura K. 17α-*O*-methylyohimbine and vallesiachotamine from roots of *Amsonia elliptica* [J]. *Phytochemistry*, 1990, **29**(10): 3377-3379.

[18] Cancelieri NM, Vieira IJC, Mathias L, *et al*. ^{1}H and ^{13}C NMR structure determination of a new stereoisomer of isoreserpiline pseudoindoxyl from *Rauvolfia grandiflora* [J]. *Magn Reson Chem*, 2003, **41**(4): 287-290.

[19] Gunatilaka AAL, Fernando HC, Atta Ur R, *et al*. Neisosposinine: a new oxindole alkaloid from *Neisosperma oppositifolia* [Apocynaceae] [J]. *Heterocycles*, 1989, **28**(2): 999-1005.

[20] Tang QQ, Lane MD. Adipogenesis: from stem cell to adipocyte [J]. *Annu Rev Biochem*, 2012, **81**: 715-736.

[21] Zeng XY, Zhou X, Xu J, *et al*. Screening for the efficacy on lipid accumulation in 3T3-L1 cells is an effective tool for the identification of new anti-diabetic compounds [J]. *Biochem Pharmacol*, 2012, **84**(6): 830-837.

[22] Kuo PL, Hsu YL, Chang CH, *et al*. The mechanism of ellipticine-induced apoptosis and cell cycle arrest in human breast MCF-7 cancer cells [J]. *Cancer Lett*, 2005, **223**(2): 293-301.

[23] Stiborová M, Frei E. Ellipticines as DNA-targeted chemotherapeutics [J]. *Curr Med Chem*, 2014, **21**(5): 575-591.

[24] Jacobsen RG, Mazloumi Gavgani F, Mellgren G, *et al*. DNA topoisomerase IIα contributes to the early steps of adipogenesis in 3T3-L1 cells [J]. *Cell Signal*, 2016, **28**(10): 1593-1603.

[25] Hsiang YH, Lihou MG, Liu LF. Arrest of replication forks by drug-stabilized topoisomerase I-DNA cleavable complexes as a mechanism of cell killing by camptothecin [J]. *Cancer Res*, 1989, **49**(18): 5077-5082.

[26] Baldwin EL, Osheroff N. Etoposide, topoisomerase II and cancer [J]. *N Curr Med Chem Anticancer Agents*, 2005, **5**(4): 363-372.

Cite this article as: XU Yao-Hao, LI Wei, RAO Yong, HUANG Zhi-Shu, YIN Sheng. Pyridocarbazole alkaloids from *Ochrosia borbonica*: lipid-lowering agents inhibit the cell proliferation and adipogenesis of 3T3-L1 adipocyte via intercalating into supercoiled DNA [J]. *Chin J Nat Med*, 2019, **17**(9): 663-671.